An All-Digital IR-UWB Transmitter with a Waveform-Synthesis Pulse Generator in 90nm CMOS for High-Density Brain Monitoring

Ali Ebrazeh and Pedram Mohseni

Electrical Engineering and Computer Science Dept, Case Western Reserve University, Cleveland, OH 44106 USA

***Abstract* — This paper reports an all-digital impulse radio ultra wideband transmitter (IR-UWB TX) fabricated in 90-nm CMOS, which incorporates a waveform-synthesis pulse generator and a timing generator for OOK/PPM pulse modulation and scrambling. The UWB pulse generator includes ten identical taps, each comprising an impulse generator and an output driver. Upon triggering by the timing generator, these taps create a programmable number of individual lobes with 4b control over their duration and amplitude, which are then combined at a shared output node to generate the UWB pulse. With a high-performance receiver, the TX might be used for moderate-data-rate (<50Mbps), m-range telemetry, suitable for brain-behavior studies, with energy consumption in the range of 12 to 20pJ/pulse, and for high-data-rate (>100Mbps), cm-range telemetry, suitable for brain-machine interfaces, with energy consumption in the range of 3.6 to 6pJ/pulse from 1.2V.**

***Index Terms* — Brain monitoring, IR-UWB transmitter, UWB pulse generator, waveform synthesis.**

I. Introduction

Electrophysiology (EPHYS) for recording action potentials from individual neurons [1] and voltammetry for sensing neurotransmitters from an ensemble of synapses [2] have been established as preferred methods for real-time monitoring of brain cellular communication at microscopic scales for investigating neural basis of behavior and pathology. More recently, time-share voltammetry and EPHYS has garnered much interest for combined, quasi-simultaneous recording of chemical and electrical neural activity from the same recording site [3].

Although microfabricated, multimodal electrode arrays have been recently developed for high-density, concurrent recording of action potentials and neurotransmitters from distributed brain areas, state-of-the-art integrated neural interfaces still face severe limitations for high-density brain monitoring in either electrical or chemical paradigm. These limitations are primarily due to elevated data rates that are difficult to support within a limited power budget (low mW-range), especially if high-density brain monitoring is conducted via conventional wireless links.

For example, the 1.1-mW, 4-channel neural recording microsystem in [3] with a 433-MHz, FSK wireless link strikes a tradeoff between functional versatility and number of available input channels. While every channel is made individually configurable for each of the three recording modalities (voltammetry, EPHYS, time-share), the resulting serial output bit stream would have had a data rate of ~23Mbps prior to any encoding, if the number of channels had been increased to 32. As another example, the *HermesE* device in [4] has an average data rate of 30Mbps for 96 channels of broadband EPHYS recording, which necessitates exploring alternative solutions for simultaneous, multichannel, wireless operation.

To address these limitations encountered with traditional, narrowband communications, pulse-based and in particular impulse radio ultra wideband (IR-UWB) transmission is becoming increasingly more popular in neural recording applications [5]-[8], enabling short-range telemetry at elevated data rates using relatively simple transmitter (TX) architectures that lend themselves to low-power, small-area implementation. This approach can potentially enable simultaneous transmission of broadband neural information on many input channels to an external receiver for further processing, obviating the need for any on-chip signal processing for online data compression.

In this paper, we describe an all-digital, highly configurable, IR-UWB TX fabricated in 90-nm, one-poly nine-metal (1P/9M) CMOS that can generate various UWB pulse shapes for use in biomedical applications that require either high-data-rate, cm-range telemetry (e.g., brain-machine interfaces in clinical neuroengineering) or moderate-data-rate, m-range telemetry (e.g., brain-behavior studies in basic neuroscience).

II. IR-UWB Transmitter Architecture

Fig. 1 shows the schematic block diagram of the all-digital IR-UWB TX, incorporating a reconfigurable pulse generator and a timing generator for pulse modulation and scrambling. The circuit is designed to directly generate FCC-compliant UWB pulses in the time domain with no need for pulse upconversion using a mixer/local oscillator [9], reducing power consumption and system complexity, or an off-chip pulse-shaping filter [10], reducing the number of external components and avoiding large attenuation of the pulse amplitude before delivery to the 50-Ω UWB antenna.

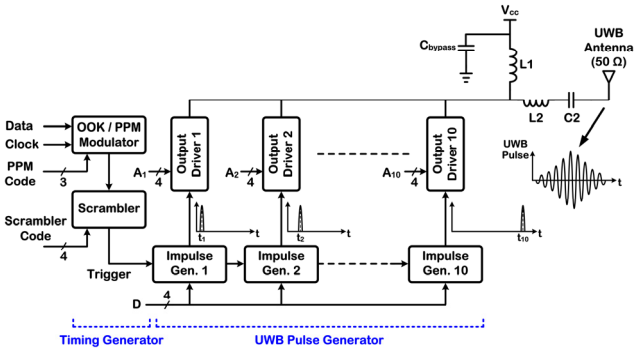

Fig. 1. Schematic block diagram of the all-digital IR-UWB TX. Inductors $L_{1,2}$ are implemented with bonding wires.

The UWB pulse generator implements a waveform-synthesis technique [11], [12] by employing ten identical taps, with each tap incorporating an impulse generator and an output driver. When the UWB pulse generator is triggered, these taps produce ten individual lobes with 4b digital control over their duration and amplitude that are then combined at a shared output node in a wired OR fashion to generate the UWB pulse waveform.

Fig. 2 depicts the circuit schematic of one individual tap of the TX. The impulse generator of the tap includes two identical delay cells with a shared 4b delay code, *D*. The first delay cell is used to generate a positive impulse by combining an input rising edge with its delayed and inverted replica using an AND gate. The output driver of the tap uses this impulse along with a 4b amplitude code, *A*, to control four binary-weighted nMOS transistors that drive the antenna. These nMOS transistors conduct within the duration of the impulse (equal to the delay of the first cell), pulling down the output node toward ground and creating the negative peak of the lobe (solid portion in Fig. 2). The second delay cell of the impulse generator provides equal time for an output resonator circuit to pull up the output node toward V_{cc} (1.2V) and create the positive peak of the lobe (dashed portion).

The output resonator circuit (see Fig. 1) comprises a pair of *LC* tanks tuned for a bandpass, wideband response around ~5GHz. Inductors $L_{1,2}$ are implemented with 25µm-diameter, gold bonding wires, whereas a thin-film capacitor (*Skyworks Solutions*) is used to implement C_2. L_1 (~1.9nH) is designed to resonate with the total capacitance of the combined output node (~0.6pF), whereas L_2 (~0.9nH) resonates with C_2 (1.2pF).

As shown in the next section, this design provides great flexibility in reconfiguring the UWB pulse waveform in the time domain (e.g., overall shape, amplitude, duration) and its power spectral density (PSD) in the frequency domain (e.g., center frequency, bandwidth, peak level).

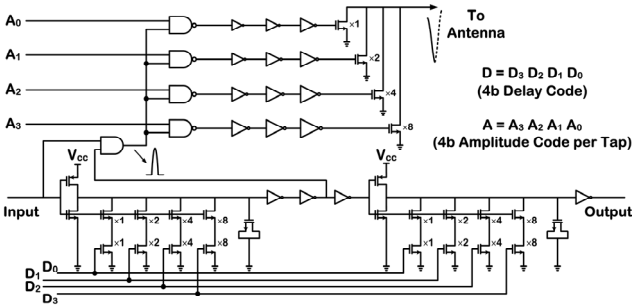

Fig. 2. Circuit schematic of one tap in the IR-UWB TX, incorporating an impulse generator (bottom) with a 4b delay code, *D*, and an output driver (top) with a 4b amplitude code, *A*.

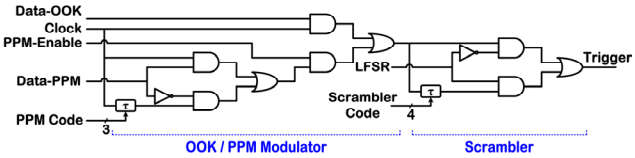

Fig. 3. Circuit schematic of the timing generator, incorporating an OOK/PPM modulator and a scrambler.

Fig. 3 depicts the circuit schematic of the timing generator used to modulate the trigger signal for pulse generation. When *PPM-Enable* is low, *Trigger* is modulated by OOK via *Data-OOK* and *Clock*. When *PPM-Enable* is high, for each bit of "0" in *Data-PPM*, *Trigger* is delayed by 3b-programmable τ_{ppm} in the range of ~ 5 to 20ns. The timing generator also incorporates a scrambler for randomizing pulse generation using a linear feedback shift register (LFSR) input. For each bit of "1" from LFSR, *Trigger* is delayed by 4b-programmable τ_{scr} equal to half of the total delay of an impulse generator.

III. Measurement Results

A prototype chip was fabricated in 90-nm 1P/9M CMOS measuring ~ 1.9 × 1.9mm^2, including the bonding pads. Fig. 4 shows a die micrograph of the fabricated chip.

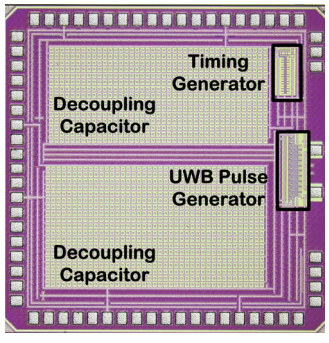

Process	90nm CMOS
Supply	1.2V
Modulation	OOK / PPM
Center Freq.	3.1 – 6GHz
PRF	≤ 500MHz
Timing Gen.	0.016mm^2
Pulse Gen.	0.045mm^2
Active Energy	3.6 – 20pJ/pulse

Fig. 4. Die micrograph of the fabricated chip.

Fig. 5 shows four different UWB pulses generated by the TX. The delay code, *D*, was set to 0111 to achieve a center frequency of ~4.65GHz, whereas the amplitude codes per tap, *A*, were specifically set as shown to achieve different pulse shapes.

Fig. 6 depicts two UWB pulses (center frequency of ~4.65GHz) generated by the TX and their measured FCC-compliant PSD for a 50-MHz pulse train with scrambling ON. Clearly, reducing the number of lobes in the waveform from 10 to 6 (by setting the corresponding amplitude codes per tap to zero) as well as reducing the amplitude of the remaining lobes widens and lowers, respectively, the resulting PSD without much variation in its center frequency. Fig. 7 depicts instead how the center frequency of the PSD can be effectively changed by adjusting the delay code, *D*.

Fig. 8 depicts the measured PSD of a 100-MHz pulse train with and without scrambling. As can be seen, the strong spectral lines, which are spaced by 100MHz and at times violate the indoor FCC mask, are effectively reduced by randomizing the trigger for pulse generation.

Fig. 9 depicts three pulse trains generated by the TX at pulse repetition frequencies (PRF) of 100, 200 and 500MHz, showing that the pulse shape and amplitude are well maintained at these high PRF values. Further, it should be noted that while a pulse waveform with 10 individual lobes is easily generated at a PRF of 100MHz, the number of lobes is reduced to two (once again by setting the corresponding amplitude codes per tap to zero) to demonstrate a PRF value as high as 500MHz.

Collectively, these results show how digital control of individual lobes within the synthesized waveform via the delay and amplitude codes enables tailoring the shape of the UWB pulse in the time domain for specific application requirements and the PSD in the frequency domain for FCC compliance, without using an external pulse-shaping filter. For example, with a high-performance receiver, the 10-lobe waveform in Fig. 9 might be used for moderate-data-rate (<50Mbps), m-range telemetry, whereas the much narrower, 2-lobe waveform might be used for high-data-rate (>100Mbps), cm-range telemetry.

Fig. 10 shows OOK and PPM modulation of the TX driven by 10b, 40-Mbps pseudo-random bit stream (PRBS) data. PPM delay (i.e., τ_{ppm}) was set to be 10ns for this measurement. The arrowheads indicate the rising edge of the sampling clock signal at the center of the bit-length.

Finally, Fig. 11 shows the plots of measured active energy consumption in pJ/pulse versus the PSD center frequency and number of lobes in the waveform. The TX energy consumption, which is primarily dominated by the current drawn from L_1 power supply (1.2V), decreases with increasing PSD center frequency due to a resulting

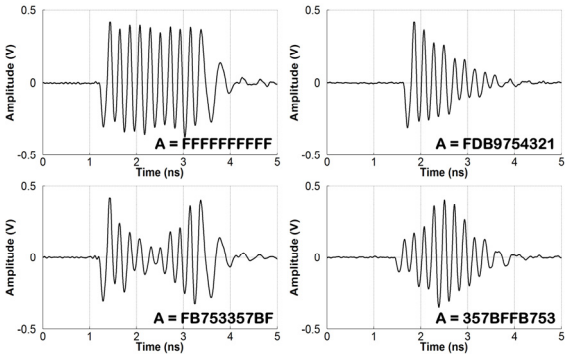

Fig. 5. Four different UWB pulses generated by the TX.

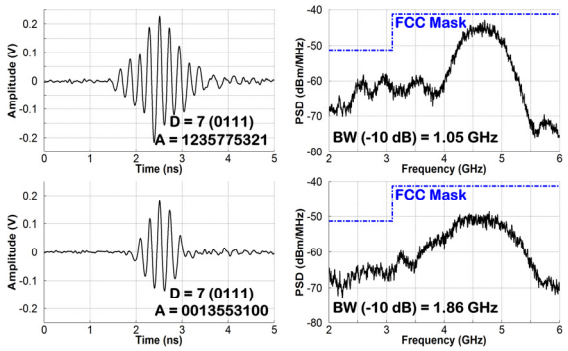

Fig. 6. Two UWB pulses generated by the TX and their corresponding FCC-compliant PSD.

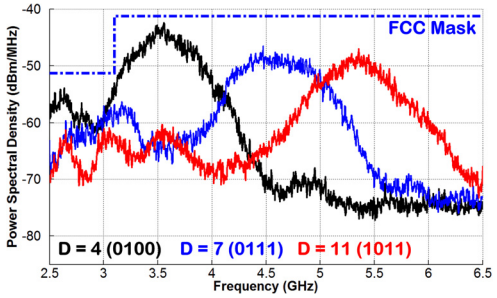

Fig. 7. PSD center frequency variation via delay code, *D*.

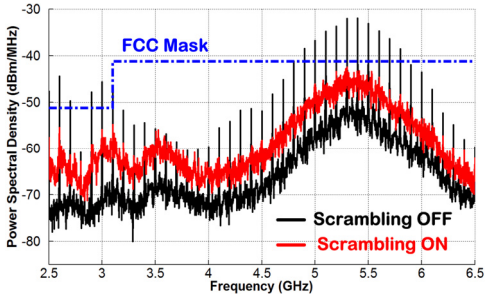

Fig. 8. Measured PSD for a 100-MHz pulse train with scrambling OFF and ON.

decrease in the pulse amplitude. For a given PSD center frequency, the active energy consumption also decreases when fewer lobes are synthesized within the waveform. Fig. 11 further suggests that it is feasible to use the TX for moderate-data-rate, m-range telemetry (e.g., in brain-behavior studies) with active energy consumption in the range of 12 to 20pJ/pulse (group 1), as well as for high-data-rate, cm-range telemetry (e.g., in brain-machine interfaces) with active energy consumption in the range of 3.6 to 6pJ/pulse (group 2).

IV. Conclusion

This paper describes an IR-UWB TX employing a waveform-synthesis pulse generator that creates highly reconfigurable UWB pulses directly in the time domain with large spectral control in the frequency domain for FCC compliance, without a need for upconversion of baseband pulses or an external pulse-shaping filter.

Acknowledgement

This work was supported by the NSF-CAREER Award DBI-0844957.

References

[1] M. Nicolelis, *Methods for Neural Ensemble Recordings*, Boca Raton, FL: CRC Press, 1999.

[2] D. L. Robinson, et al., "Monitoring rapid chemical communication in the brain," *Chem. Rev.*, vol. 108, pp. 2554-2584, 2008.

[3] M. Roham, D. P. Covey, D. P. Daberkow, E. S. Ramsson, C. D. Howard, B. A. Heidenreich, P. A. Garris, and P. Mohseni, "A wireless IC for time-share chemical and electrical neural recording," *IEEE J. Solid-State Circuits*, vol. 44, no. 12, pp. 3645-3658, December 2009.

[4] H. Gao, et al., "HermesE: A 96-channel full data rate direct neural interface in 0.13µm CMOS," *IEEE J. Solid-State Circuits*, vol. 47, no. 4, pp. 1043-1055, April 2012.

[5] F. Inanlou, M. Kiani, and M. Ghovanloo, "A 10.2 Mbps pulse harmonic modulation based transceiver for implantable medical devices," *IEEE J. Solid-State Circuits*, vol. 46, no. 6, pp. 1296-1306, June 2011.

[6] E. Greenwald, et al., "A VLSI neural monitoring system with ultra-wideband telemetry for awake behaving subjects," *IEEE Trans. Biomed. Circuits and Systems*, vol. 5, no. 2, pp. 112-119, April 2011.

[7] H. Miranda and T. H. Meng, "A programmable pulse UWB transmitter with 34% energy efficiency for multichannel neuro-recording systems," in *Proc. Custom Integr. Circ. Conf. (CICC'10)*, pp. 1-4, September 2010.

[8] M. S. Chae, et al., "A 128 channel 6 mW wireless neural recording IC with spike feature extraction and UWB transmitter," *IEEE Trans. Neural Syst. Rehab. Eng.*, vol. 17, no. 4, pp. 312-321, August 2009.

[9] H. Hedayati and K. Entesari, "A 3.1-10.6 GHz ultra-wide band impulse radio transmitter with notch implementation for in-band interferers in 90nm CMOS," in *Proc. RF Integr. Circ. Symp. (RFIC'12)*, pp. 459-462, June 2012.

[10] Y. Park and D. D. Wentzloff, "An all-digital 12 pJ/pulse IR-UWB transmitter synthesized from a standard cell library," *IEEE J. Solid-State Circuits*, vol. 46, no. 5, pp. 1147-1157, May 2011.

[11] Y. Zhu, et al., "Distributed waveform generator: A new circuit technique for ultra-wideband pulse generation, shaping and modulation," *IEEE J. Solid-State Circuits*, vol. 44, no. 3, pp. 808-823, March 2009.

[12] V. V. Kulkarni, et al., "A 750 Mbps, 12 pJ/b, 6-to-10 GHz CMOS IR-UWB Transmitter with embedded on-chip antenna," *IEEE J. Solid-State Circuits*, vol. 44, no. 2, pp. 394-403, February 2009.

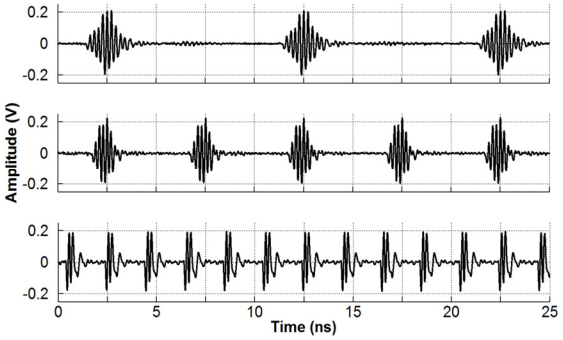

Fig. 9. Generated pulse waveforms at 100, 200 and 500MHz.

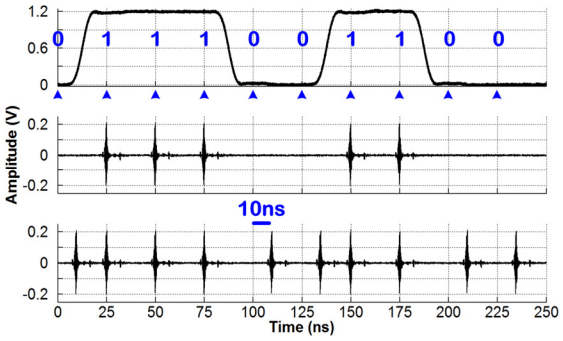

Fig. 10. OOK (middle) and PPM (bottom) modulation of the IR-UWB TX using 10b, 40-Mbps PRBS data (top).

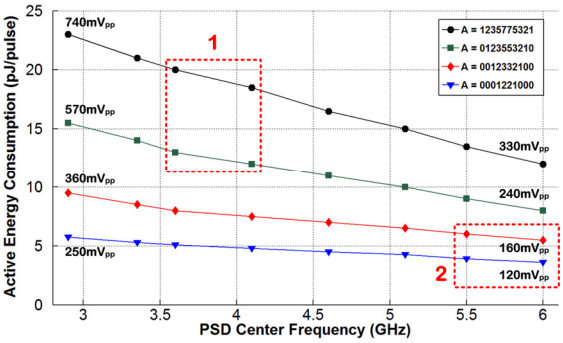

Fig. 11. Active energy consumption per pulse generation *vs.* PSD center frequency and number of lobes within the waveform.